Cell Reports

Report

A Recombinant Antibody-Expressing Influenza Virus Delays Tumor Growth in a Mouse Model

Graphical Abstract

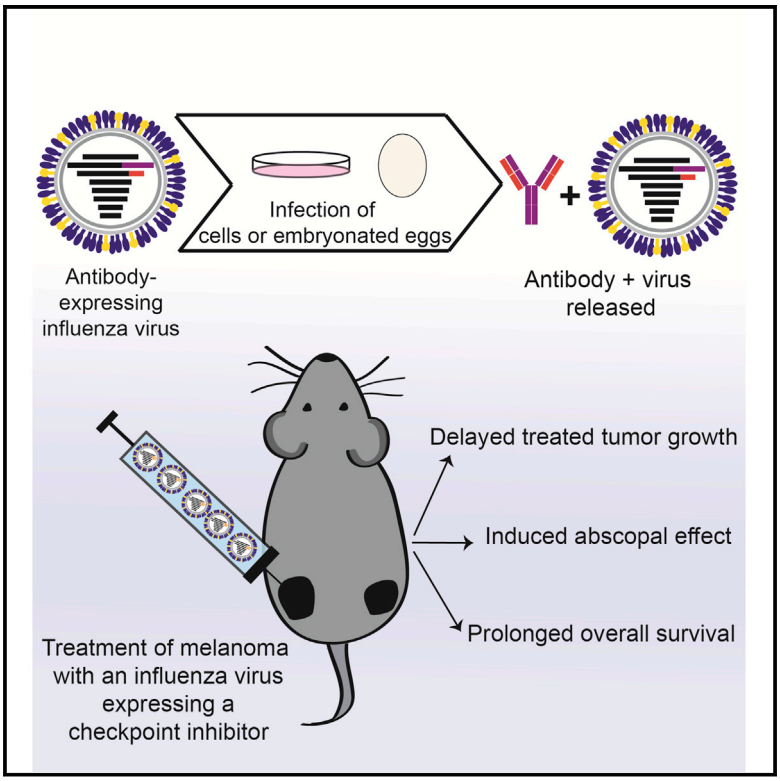

Highlights

- Influenza A viruses expressing full and single-chain antibodies are generated
- Antibody-expressing influenza viruses replicate well *in vitro* and *in vivo*
- Intratumoral treatment with CTLA4-blocking influenza virus limits melanoma growth
- CTLA4-blocking influenza virus drives an abscopal effect and prolongs survival

Authors

Jennifer R. Hamilton,
Gayathri Vijayakumar, Peter Palese

Correspondence

peter.palese@mssm.edu

In Brief

Influenza virus has potential as an anti-cancer agent. Hamilton et al. engineer antibody-expressing influenza viruses and demonstrate that encoding a single-chain antibody blocking the immune checkpoint CTLA4 enhances the anti-cancer activity of influenza virus. These data suggest a strategy for improving the oncolytic nature of *Orthomyxoviruses.*

Hamilton et al., 2018, Cell Reports *22*, 1–7
January 2, 2018
https://doi.org/10.1016/j.celrep.2017.12.025

CellPress

Cell Reports
Report

A Recombinant Antibody-Expressing Influenza Virus Delays Tumor Growth in a Mouse Model

Jennifer R. Hamilton,[1] Gayathri Vijayakumar,[1] and Peter Palese[1,2,3,*]
[1]Department of Microbiology, Icahn School of Medicine at Mount Sinai, New York, NY 10029, USA
[2]Department of Medicine, Icahn School of Medicine at Mount Sinai, New York, NY 10029, USA
[3]Lead Contact
*Correspondence: peter.palese@mssm.edu
https://doi.org/10.1016/j.celrep.2017.12.025

SUMMARY

Influenza A virus (IAV) has shown promise as an oncolytic agent. To improve IAV as an oncolytic virus, we sought to design a transgenic virus expressing an immune checkpoint-inhibiting antibody during the viral life cycle. To test whether it was possible to express an antibody during infection, an influenza virus was constructed encoding the heavy chain of an antibody on the PB1 segment and the light chain of an antibody on the PA segment. This antibody-expressing IAV grows to high titers, and the antibodies secreted from infected cells exhibit comparable functionality with hybridoma-produced antibodies. To enhance the anti-cancer activity of IAV, an influenza virus was engineered to express a single-chain antibody antagonizing the immune checkpoint CTLA4 (IAV-CTLA4). In mice implanted with the aggressive B16-F10 melanoma, intratumoral injection with IAV-CTLA4 delayed the growth of treated tumors, mediated an abscopal effect, and increased overall survival.

INTRODUCTION

Oncolytic viruses have demonstrated potential as a treatment agent for advanced melanoma (Andtbacka et al., 2015). The efficacy of oncolytic viruses relies on two predominant mechanisms: (1) the direct killing of infected tumor cells; and (2) the ability to provoke a systemic, anti-tumor immune response that mediates the clearance of non-infected tumor cells (Russell et al., 2012). In 2015, oncolytic virus therapy was approved in the United States. Recently, the oncolytic virus talimogene laherparepvec (T-VEC) was tested in combination with the anti-CTLA4 checkpoint inhibitor antibody ipilimumab in a phase 1b trial; combination therapy was demonstrated to be safe and seemed to enhance efficacy (Chesney et al., 2016; Puzanov et al., 2016). Moreover, it has been established that T-VEC + ipilimumab combination therapy is more effective than ipilimumab alone (Chesney et al., 2017).

While combining two immunotherapy agents is an attractive strategy to support an anti-cancer immune response, systemic delivery of checkpoint inhibitors has been associated with adverse autoimmune responses (Bertrand et al., 2015; Weber, 2007). To circumvent this obstacle, it has been shown that the response to low-dose, intratumoral administration of checkpoint inhibitors is comparable to systemic, high-dose delivery (Fransen et al., 2013; Sandin et al., 2014; Simmons et al., 2008; Tuve et al., 2007) and that the expression of checkpoint inhibitors directly from oncolytic viruses is a viable strategy to promote a tumor-specific immune response (Bartee et al., 2017; Dias et al., 2012; Engeland et al., 2014; Kleinpeter et al., 2016).

Influenza A virus (IAV) has long been studied as an oncolytic virus (Lindenmann and Klein, 1967; Moore, 1949). Moreover, the tumor-targeting ability of IAV has been enhanced through the inactivation of the IAV protein responsible for interferon antagonism, NS1 (Bergmann et al., 2001; Efferson et al., 2006; Muster et al., 2004), and through the manipulation of the host immune response via cytokine expression (Hock et al., 2017; van Rikxoort et al., 2012). Influenza viruses expressing transgenes from the polymerase segments have been described previously (Fulton et al., 2015; Heaton et al., 2013; Pena et al., 2013; Tran et al., 2013), although this strategy has not been employed to express more than one transgene from the same virus. As a proof of concept, this report describes a replication-competent IAV that utilizes the PB1 and PA viral polymerase segments to express a well-characterized antibody that targets group 2 IAV hemagglutinins. In addition, this strategy was used to express an anti-CTLA4 checkpoint inhibitor, which enhances the oncolytic potential of IAV in a mouse melanoma model.

RESULTS

Design and Rescue of an Antibody-Expressing IAV

To engineer a replication-competent IAV that expresses antibodies during the viral life cycle, the polymerase PB1 and PA segments were utilized. To assess the feasibility of antibody expression by IAV, genes for the well-characterized antibody 9H10 (Tan et al., 2014) were first encoded into the A/Puerto Rico/8/34 (PR8) IAV background. The 9H10 antibody binds the stalk region of group 2 hemagglutinins (such as the H3 of the X-31 virus) and does not bind group 1 viruses, such as PR8 (Tan et al., 2014).

To express the 9H10 antibody from IAV, both the heavy- and light-chain genes were inserted into the IAV genome (Figure 1A). The heavy-chain gene was cloned downstream of PB1. The Porcine teschovirus 1 (PTV-1) 2A sequence was inserted between the PB1 and heavy-chain genes to allow for the co-translational

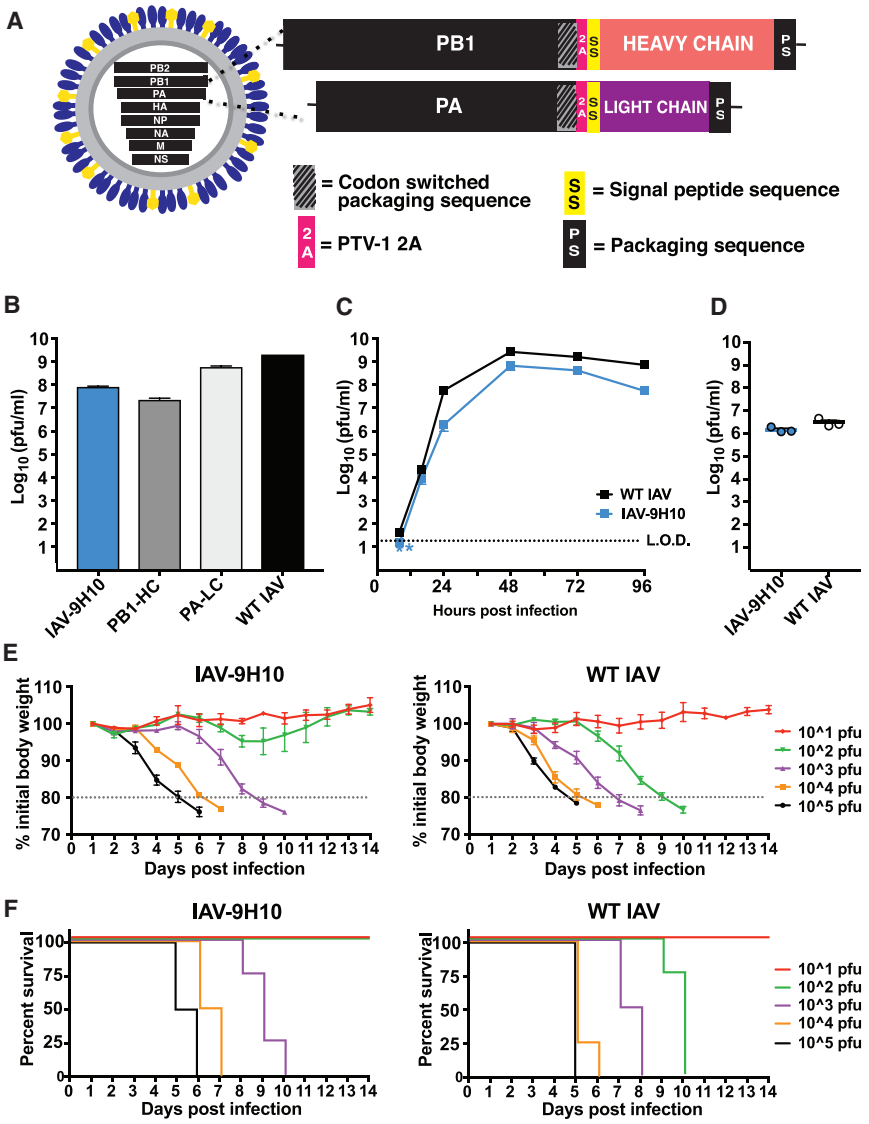

Figure 1. *In Vitro* and *In Vivo* Growth Characteristics of IAV-9H10

(A) Diagram of IAV engineered to express antibodies during infection.

(B) Peak titer following viral growth in eggs at 33°C for 3 days. IAV-9H10 (harboring both PB1-9H10$_{heavy\ chain}$ and PA-9H10$_{light\ chain}$ segments) viruses containing single transgenic segments and WT IAV are shown. HC, heavy chain; LC, light chain.

(C) Viral growth in eggs, 5 eggs per time point per virus. *Samples below the limit of detection (LOD).

(D) Viral lung titers 2 days post intranasal infection with 5 × 10^5 PFUs of IAV-9H10 or WT IAV (n = 3 mice per group).

(E and F) Following infection, (E) body weight loss and (F) survival were quantified (n = 4 mice per group). Experiments were performed in duplicate and all error bars represent SEM. Diagram is not to scale.

separation of the PB1 and heavy-chain proteins. Additionally, a signal peptide sequence was cloned between the 2A and the heavy-chain sequence to target the nascent heavy-chain polypeptide for translation into the endoplasmic reticulum and subsequent secretion. The same strategy was employed to direct light-chain expression from the viral PA segment.

An IAV expressing both PB1-9H10$_{heavy\ chain}$ and PA-9H10$_{light\ chain}$ segments was rescued (IAV-9H10), as well as viruses expressing either of the transgenic segments alone. All viruses grew to high titer, with IAV-9H10 reaching ~1 × 10^8 plaque-forming units (PFUs)/mL, an approximate 1 $\log_{10}$ reduction in peak titer compared to wild-type (WT) IAV (Figure 1B). Moreover, the multicycle replication kinetics of IAV-9H10 closely mimicked that of WT IAV (Figure 1C).

Additionally, the capability of IAV-9H10 to replicate *in vivo* was assessed. Intranasal infection of mice with IAV-9H10 resulted in both high viral lung titers (Figure 1D) and weight loss-associated morbidity and mortality (Figures 1E and 1F). The dose at which 50% of the mice succumbed to infection was $10^{1.5}$ PFUs for WT IAV and $10^{2.5}$ PFUs for IAV-9H10, a minimal attenuation that is similar to that of recombinant PR8 viruses harboring a single transgenic polymerase segment (Heaton et al., 2013). Together, it can be concluded that encoding both antibody genes into the IAV genome minimally affects viral growth and virulence *in vivo*.

Antibody Is Produced during IAV-9H10 Infection

We next sought to address the production of antibody during IAV-9H10 infection. First, RT-PCR was used to establish that viral IAV-9H10 stocks contained transgenic segments of the expected size. The terminal 300 nt of WT IAV PB1 and PA, or 1,902 and 1,194 nt for the transgenic segments, respectively, was amplified (Figure 2A). Next, we assessed the kinetics of antibody production during IAV-9H10 infection. Eggs were inoculated with IAV-9H10, and the amount of antibody present in the allantoic fluid was quantified; antibody was detectable 2 days following inoculation and peaked at 4–5 days (Figure 2B).

The transgenes encoded by IAV-9H10 are relatively large: 1,605 additional nt is encoded on the PB1 segment and 897 nt is encoded on the PA segment. Because of these large insertions, we next addressed the stability of antibody expression over time. Passaging of IAV-9H10 was performed in eggs and functional transgene expression was assessed. Dilutions and viral amplifications were repeated for a total of four passages, and no loss in the quantity of antibody produced was observed (Figure 2C), suggesting that the antibody genes are stably maintained in the IAV genome.

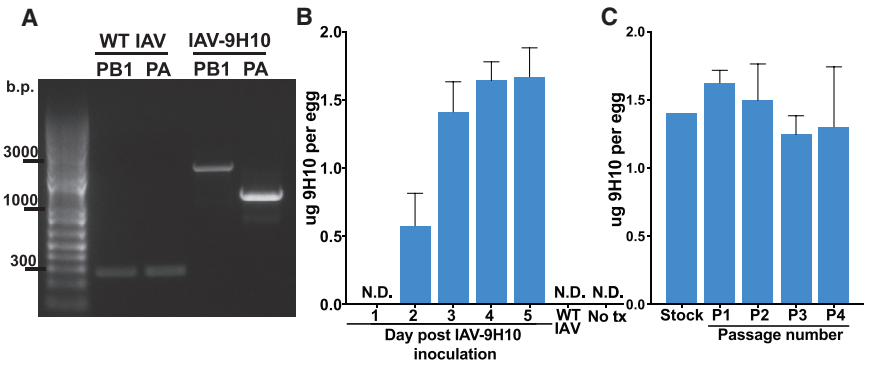

Figure 2. Antibody Is Produced during IAV-9H10 Infection *In Ovo*

(A) Detection of transgenic segments in IAV-9H10. Viral RNA was isolated and RT-PCR was performed to amplify the terminal 300 bp of WT PB1 or PA. The expected PCR products for the IAV-9H10 PB1 and PA are 1,902 and 1,194 bp, respectively.

(B) 9H10 quantity following inoculation with ~10 PFUs, 3–4 eggs per time point, and assessed via ELISA. Eggs inoculated with WT IAV were assessed on day 3. ND, not detected.

(C) Antibody expression is stable during passaging of IAV-9H10 in eggs. IAV-9H10 was diluted 10^{-6} and 100 μL was used to inoculate 3 eggs (passage 1 [P1]). Following viral growth at 33°C for 3 days, allantoic fluid was isolated, diluted 10^{-6}, and injected back into 3 eggs. This was repeated for a total of 4 passages; 9H10 was quantified via ELISA.

(B) and (C) were performed in duplicate and error bars represent SEM. No tx, no treatment.

Antibody Produced in Eggs Functions in *In Vitro* and *In Vivo* Assays

To address whether IAV-produced antibody functions like an antibody produced via hybridoma technology, 9H10 antibody was concentrated from the allantoic fluid of IAV-9H10-infected eggs. Both IAV-produced and hybridoma-produced antibody performed equally well for *in vitro* and *in vivo* assays. $9H10_{IAV}$ and $9H10_{hybridoma}$ bound equivalently in an X-31 ELISA (Figure 3A), and both aliquots worked to inhibit the infection of Madin Darby canine kidney (MDCK) cells when pre-incubated with X-31 (Figure 3B). Additionally, mice administered prophylaxis $9H10_{IAV}$ and $9H10_{hybridoma}$ prior to X-31 challenge were protected from infection-induced morbidity (Figure 3C) and mortality (Figure 3D).

Characterizing the IAV Infection of B16-F10 Melanoma Cells

We reasoned that an influenza virus expressing an antibody antagonizing an immune checkpoint would augment the oncolytic activity of IAV for treating melanoma cancer *in vivo*. However, IAV infection of melanoma cells first needed to be characterized. *In vitro*, B16-F10 cells were susceptible to virus-induced cell death, and no difference in cell death was observed between WT IAV and IAV-9H10-infected cells (Figure 4A). Moreover, antibody was produced from B16-F10 cells infected with IAV-9H10 (Figure 4B). It was possible to reduce cell viability to below 5% if tolylsulfonyl phenylalanyl chloromethyl ketone (TPCK)-trypsin was added to the media following infection, suggesting that B16-F10 cells do not express the proteases necessary for multicycle viral growth (data not shown). Indeed, IAV did not have the capacity to initiate multicycle replication in B16-F10 melanoma cells in the absence of trypsin, and addition of the protease resulted in high viral titers (Figure 4C). This potentially enhances the safety profile of influenza virus as an oncolytic for trypsin-deficient tumors, as uncontrolled viral replication would not be possible.

Treatment of B16-F10 Melanoma Tumors with IAV-CTLA4 Delayed Tumor Growth and Prolonged Overall Survival

To encode an antibody that mediates a checkpoint blockade, we utilized a publicly available sequence for the 9D9 single-chain variable fragment (scFv) targeting mouse CTLA4 (Allison and Curran, 2011). The 9D9 scFv was cloned into both the PB1 and PA segments, using the strategy described in Figure 1, and rescued in the PR8 background. A bilateral flank tumor model was used to assess the activity of IAV-CTLA4: B16-F10 cells were implanted into both the right and left rear flanks of mice. Only the right flank tumors were treated, and the left flank tumors were monitored to assess an abscopal effect mediated by the host anti-tumor immune response (Figure 4D).

Right-flank tumors received four intratumoral injections, spaced 48 hr apart, and tumor growth was measured every 2 days. Treatment with WT IAV slowed the growth of right flank tumors, compared to mice receiving PBS injections; however, mice administered IAV-CTLA4 demonstrated minimal growth of the treated tumor (Figure 4E). Additionally, IAV-CTLA4-treated mice exhibited delayed growth of untreated, left flank tumors, suggesting that IAV-CTLA4 treatment was supporting a systemic anti-tumor immune response (Figure 4F). Importantly, IAV-CTLA4 treatment led to prolonged survival compared to mice administered WT IAV or PBS alone (Figure 4G).

DISCUSSION

Oncolytic viruses have demonstrated potential as anti-cancer agents both in the laboratory and in the clinic. Current development focuses on honing the tumor specificity of oncolytic viruses, as well as promoting the activation of the adaptive immune system and a systemic, anti-tumor response.

This paper demonstrates that IAV can be engineered to express antibodies. IAV-expressed antibodies are secreted from infected cells and are detectable in both the supernatant of infected cells and the allantoic fluid of infected eggs. IAV-expressed antibody was found to be functional in both *in vitro* ELISA and microneutralization assays, as well as in prophylaxis protection studies *in vivo*. The functionality of IAV-expressed antibody may vary depending on the antibody expressed. Herein, we have studied the 9H10 antibody, which is predicted to contain one N-linked glycosylation site in the constant region of the heavy chain. As the influenza neuraminidase cleaves sialic acid residues, this may potentially interfere with the glycosylation of antibodies expressed during infection.

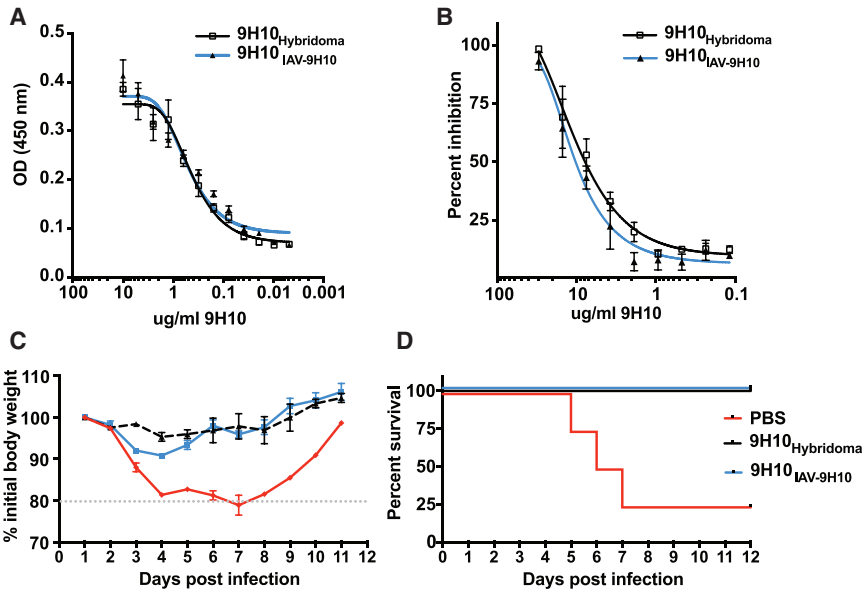

Figure 3. Antibody Produced during IAV-9H10 Infection *In Ovo* Is Functional

(A) ELISA assessing the binding of 9H10 to X-31 virus. Antibodies were diluted to 10 μg/mL, and 2-fold dilutions were performed in triplicate. OD, optical density.

(B) Microneutralization assay comparing IAV-produced and hybridoma-produced 9H10 antibody. Both aliquots protect MDCK cells from infection with X-31.

(C and D) Intranasal treatment with 10 μg 9H10 24 hr prior to infection protects mice from (C) morbidity and (D) mortality following X-31 challenge with 3× LD50 (n = 4 mice per group). Both $9H10_{hybridoma}$ and $9H10_{IAV\text{-}9H10}$ protect mice from challenge. All experiments were performed in duplicate and error bars represent SEM.

Regardless, in this report the activity of IAV-expressed 9H10 was as expected.

This report demonstrates that the oncolytic activity of IAV is enhanced through the expression of a single-chain variable fragment targeting the immune checkpoint CTLA4. B16-F10 melanoma is a highly aggressive and metastatic model of cancer known for its rapid growth *in vivo* (Kuzu et al., 2015; Overwijk and Restifo, 2001). Intratumoral injection with IAV-CTLA4 resulted in the potent growth inhibition of B16-F10 tumors. Moreover, treatment with IAV-CTLA4 mediated an abscopal effect, delaying the growth of distal, untreated tumors, as well as prolonging overall survival. Future studies will be necessary to determine whether the oncolytic activity of IAV-CTLA4 is restricted to B16-F10 melanoma or if it is broadly applicable to other tumor models.

Previous work with oncolytic Newcastle disease virus (NDV) has demonstrated that virus does not spread between the injected and non-injected contralateral tumors (Zamarin et al., 2014). The requirements for receptor usage and multicycle viral growth are shared between NDV and IAV. Moreover, the systemic spread of H1N1 IAV has not been observed in animal models (Belser et al., 2010; Heaton et al., 2013). Together, we do not expect IAV-CTLA4 to spread and directly replicate in uninjected tumors. Instead, we hypothesize that there are tumor-specific CD8+ T cells at the site of the tumors injected with IAV-CTLA4 and that expression of a checkpoint inhibitor by infected tumor cells potentiates their cytotoxic activity. This strategy of checkpoint inhibitor expression at the site of a tumor may favor the activation of tumor-specific T cells, compared to systemic delivery of checkpoint inhibitor. However, more work has to be done to demonstrate that this is the mechanism mediating the abscopal effect in IAV-CTLA4-treated mice and to determine if the abscopal effect is tumor type specific (as has been observed with oncolytic NDV; Zamarin et al., 2014). Additional studies will further assess whether IAV expression of checkpoint inhibitors is safer than intravenous (i.v.) administration.

IAV is an attractive oncolytic candidate because, as an RNA virus, it is incapable of integration into the host genome. Previous research on oncolytic influenza viruses has focused on utilizing NS1-deficient viruses as oncolytic agents (Bergmann et al., 2001; Efferson et al., 2006; Muster et al., 2004). NS1 is responsible for interferon antagonism during IAV infection, and it is essential for replication in interferon-competent cells (García-Sastre et al., 1998). It has been demonstrated that NS1-deficient IAVs are capable of replicating in ras-expressing tumor cells (Bergmann et al., 2001), as well those deficient for interferon production. It will be valuable to compare the oncolytic activity of antibody-expressing IAV with and without NS1; it may be that the injection of IAV directly into melanoma tumors is sufficient to target the virus to preferentially infect tumorous cells and, therefore, does not necessitate NS1 attenuation.

In summary, we have used an antibody-expressing IAV as an anti-cancer agent. IAV-CTLA4 treatment limited melanoma tumor growth and prolonged survival time. The minimal attenuation of the antibody-expressing IAV suggests that the IAV genome may be capable of tolerating the insertion of even larger transgenes. While this paper has focused on the oncolytic capabilities of an antibody-expressing IAV, this platform may further be useful for the *in vitro* evolution of antibodies or as a mechanism for directing the expression of beneficial monoclonal antibodies in the upper respiratory tract of IAV-infected individuals.

EXPERIMENTAL PROCEDURES

Cell Lines and Viruses

293T, B16-F10, and MDCK cells were used in this study (ATCC). 293T cells were maintained in DMEM, B16-F10 cells were maintained in DMEM:F12, and MDCK cells were maintained in Eagle's minimal essential medium (EMEM, Gibco). Media were supplemented with 10% fetal bovine serum (FBS) and penicillin/streptomycin. PR8, X-31, IAV-9H10, and IAV-CTLA4 viruses were grown in 10-day-old specific pathogen-free (SPF) chicken eggs (Charles River Laboratories).

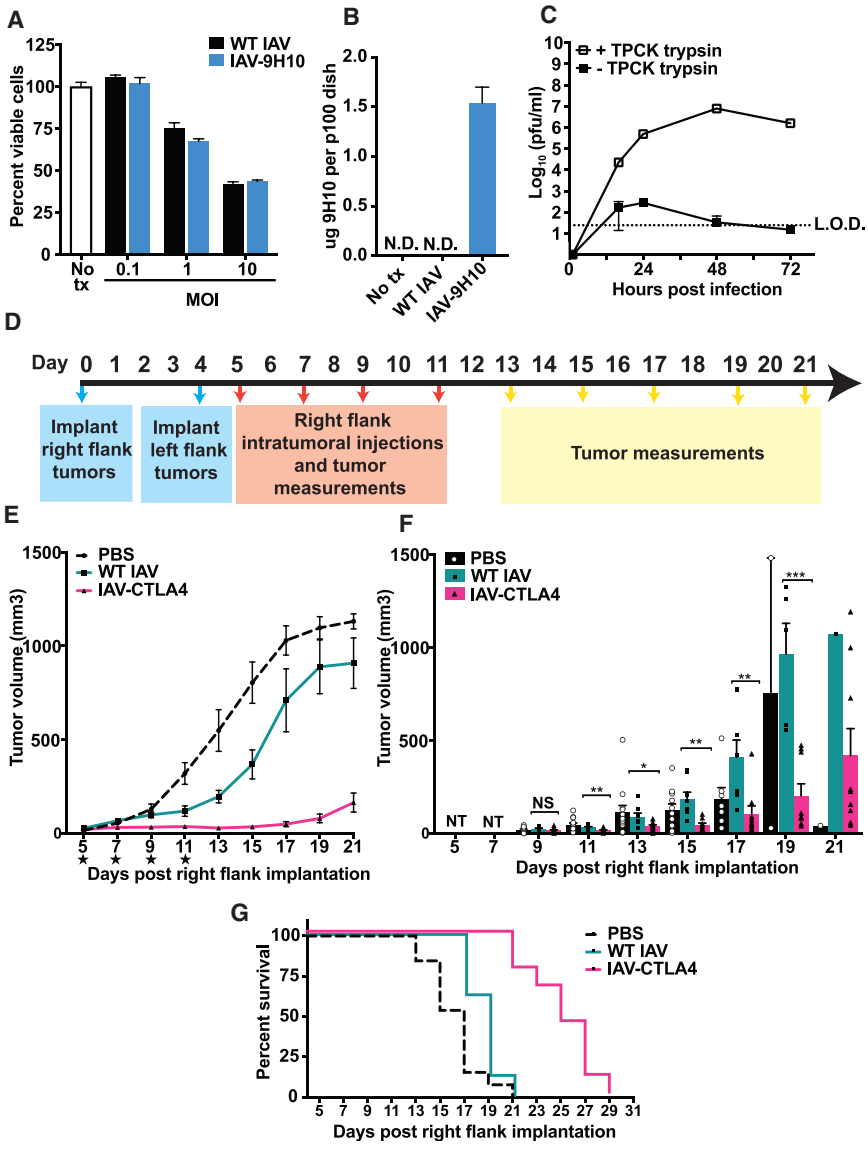

Figure 4. IAV-CTLA4 Delays Growth of B16-F10 Melanoma Tumors *In Vivo* and Prolongs Overall Survival

(A) B16-F10 cells undergo cell death *in vitro* following infection with WT IAV or IAV-9H10. Viability was assayed 48 hpi in quadruplicates and normalized to uninfected cells.

(B) B16-F10 cells secrete antibody following IAV-9H10 infection at MOI = 5; 9H10 was quantified 48 hpi in triplicate via ELISA. ND, not detected.

(C) B16-F10 cells do not support multicycle replication in the absence of TPCK-trypsin. Cells were infected at MOI = 0.01 with WT IAV, incubated ±TPCK-trypsin, and virus titrated in triplicate.

(D) Experimental timeline for the assessment of IAV-CTLA4 as an oncolytic agent. B16-F10 cells were implanted in the right flank on day 0 and in the left flank on day 4. Right-flank tumors were intratumorally injected with WT IAV or IAV-CTLA4 (5.5×10^5 PFUs/injection) or PBS on days 5, 7, 9, and 11. From day 13 onward, tumor volumes were measured every 2 days.

(E) Right-flank tumors treated with IAV-CTLA4 demonstrate delayed growth compared to PBS- and IAV WT-treated tumors. Mice with tumors exceeding 1,000 mm^3 were sacrificed, and their last-measured tumor volumes were used for subsequent tumor measurements. Stars indicate when mice received right-flank intratumoral injections (n = 13, n = 8, and n = 9 mice per PBS, WT IAV, and IAV-CTLA4 groups, respectively).

(F) An abscopal effect is induced by IAV-CTLA4 treatment. Left-flank, untreated tumors of mice administered IAV-CTLA4 demonstrate a delayed growth, compared to mice treated with WT IAV. NT, not tested; NS, not significant. Statistical analysis was performed using unpaired, two-tailed Student's t tests (*$p \leq 0.05$, **$p \leq 0.01$, and ***$p \leq 0.001$). Symbols indicate individual tumor volumes; note that on day 21 only one mouse remained in each of the PBS and WT IAV groups. For (E) and (F), data are shown until all PBS and WT IAV mice developed tumors >1,000 mm^3.

(G) IAV-CTLA4 treatment prolongs overall survival. LOD, limit of detection. Experiments were performed in duplicate and error bars represent SEM.

Plasmids and Rescue of Recombinant Antibody-Expressing Influenza Viruses

$PB1\text{-}9H10_{heavy\ chain}$, $PA\text{-}9H10_{light\ chain}$, $PB1\text{-}9D9_{ScFv}$, and $PA\text{-}9D9_{ScFv}$ sequences were cloned into the ambisense cloning vector pDZ, as previously described (Grimm et al., 2007), and sequenced prior to viral rescue. See the Supplemental Experimental Procedures for further details.

Viability Assays

Viability of B16-F10 cells following IAV infection was quantified 48 hr post infection (hpi) using Cell Titer Glo (Promega), as described in the Supplemental Experimental Procedures.

RT-PCR and vRNA Isolation

Viral RNA (vRNA) was extracted and RT-PCR was performed to amplify the terminal 300 nt of WT PB1 and PA segments. Because of transgene insertion, the predicted sizes of $PA\text{-}9D9_{light\ chain}$ and $PB1\text{-}9D9_{ScFv}$ transgenic segments are 1,902 and 1,194 bp, respectively. Additional details and primer sequences can be found in the Supplemental Experimental Procedures.

Purification of Antibodies

Hybridoma-produced antibody was isolated as described previously (Tan et al., 2014). To isolate 9H10 from IAV-9H10-infected eggs, eggs were inoculated, incubated at 33°C for 3–4 days, and allantoic fluid was pooled. 9H10 was concentrated using Protein G, as detailed in the Supplemental Experimental Procedures.

ELISA and Microneutralization Assay

ELISAs were performed as previously described (Hamilton et al., 2016) and are detailed in the Supplemental Experimental Procedures. The quantity of 9H10 antibody per egg was calculated by multiplying the total volume of allantoic fluid per egg by the concentration of the antibody.

Microneutralization assays were performed by mixing diluted antibody with X-31 prior to incubation with MDCK cells. Following incubation, the virus/antibody mix was replaced with media containing the appropriate antibody dilution. Infection was detected and analyzed as described previously (He et al., 2015). More details are provided in the Supplemental Experimental Procedures.

Viral Infections

Eggs were inoculated with 100 PFUs IAV-9H10 or WT IAV for *in ovo* viral growth curves. For *in vitro* growth curves, B16-F10 cells were infected with WT IAV, MOI = 0.01, ±TPCK-trypsin at 1 μg/mL (Sigma). For the detection of antibody following a single-cycle viral infection *in vitro*, B16-F10 cells were infected with IAV-9H10 for 48 hr, MOI = 5. All viral samples were titrated via standard plaque assay on MDCK cells. More details are provided in the Supplemental Experimental Procedures.

Animal Experiments

Female C57BL/6 mice were purchased (Jackson ImmunoResearch Laboratories), and all animal experiments were performed in accordance with the Icahn School of Medicine at Mount Sinai Animal Care and Use Committee.

For tumor studies, 4- to 6-week-old mice were anesthetized by intraperitoneal (i.p.) injections of ketamine/xylazine, and 2×10^5 B16-F10 cells were implanted intradermally on the right flank, and then 4 days later 1×10^5 cells were implanted on the left flank. Tumor progression was measured every 48 hr starting at 5–6 days post-right flank implantation. Right-flank tumors were injected with 5.5×10^5 PFUs WT IAV or IAV-CTLA4 diluted to 100 μL in PBS on days 5, 7, 9, and 13. Mice were sacrificed when tumors exceeded 1,000 mm^3, and their last-measured tumor volumes were used for subsequent right-flank tumor measurements. Mice with right-flank tumors >40 mm^3 on day 5 and mice that developed intramuscular tumors were excluded from the study.

Intranasal influenza virus infections were performed using 6- to 8-week-old mice, as described previously (Hamilton et al., 2016), and mice were sacrificed when reaching 80% of their starting body weight. Viral lung titer quantification was also described previously (Hamilton et al., 2016).

For *in vivo* protection studies, mice were anesthetized with ketamine/xylazine and administered 10 μg 9H10 in 40 μL PBS 24 hr prior to intranasal infection with 3× LD50 X-31. During prophylactic treatment, all groups also received the anti-PR8 hemagglutinin (HA) antibody PY102 at a final concentration of 30 μg/mL in order to neutralize any IAV-9H10 virus that was present in the $9H10_{IAV}$ antibody aliquot.

Statistical Analysis

Unpaired, two-tailed Student's t tests were used to calculate significance with $p \leq 0.05$ considered significant (Prism, GraphPad).

SUPPLEMENTAL INFORMATION

Supplemental Information includes Supplemental Experimental Procedures and can be found with this article online at https://doi.org/10.1016/j.celrep.2017.12.025.

ACKNOWLEDGMENTS

The authors would like to thank Mr. Mark Bailey and Dr. Gene Tan for providing sequences and reagents and for their helpful discussions regarding experimental design. The authors would also like to thank Dr. Sara Cuadrado for assistance with tumor implantation. This work was partially supported by F31AI120648 (J.R.H.).

AUTHOR CONTRIBUTIONS

J.R.H., G.V., and P.P. designed the research. J.R.H. and G.V. performed the research. J.R.H. analyzed data and J.R.H. and P.P. wrote the paper.

DECLARATION OF INTERESTS

The authors declare no competing interests.

Received: October 11, 2017
Revised: November 9, 2017
Accepted: December 6, 2017
Published: January 2, 2018

REFERENCES

Allison J., and Curran, M. (2011). Methods and Compositions for Localized Secretion of Anti-CTLA-4 Antibodies. US patent US20110044953 A1, filed March 30, 2007, and published February 24, 2011.

Andtbacka, R.H.I., Kaufman, H.L., Collichio, F., Amatruda, T., Senzer, N., Chesney, J., Delman, K.A., Spitler, L.E., Puzanov, I., Agarwala, S.S., et al. (2015). Talimogene Laherparepvec Improves Durable Response Rate in Patients With Advanced Melanoma. J. Clin. Oncol. *33*, 2780–2788.

Bartee, M.Y., Dunlap, K.M., and Bartee, E. (2017). Tumor-Localized Secretion of Soluble PD1 Enhances Oncolytic Virotherapy. Cancer Res. *77*, 2952–2963.

Belser, J.A., Wadford, D.A., Pappas, C., Gustin, K.M., Maines, T.R., Pearce, M.B., Zeng, H., Swayne, D.E., Pantin-Jackwood, M., Katz, J.M., and Tumpey, T.M. (2010). Pathogenesis of pandemic influenza A (H1N1) and triple-reassortant swine influenza A (H1) viruses in mice. J. Virol. *84*, 4194–4203.

Bergmann, M., Romirer, I., Sachet, M., Fleischhacker, R., García-Sastre, A., Palese, P., Wolff, K., Pehamberger, H., Jakesz, R., and Muster, T. (2001). A genetically engineered influenza A virus with ras-dependent oncolytic properties. Cancer Res. *61*, 8188–8193.

Bertrand, A., Kostine, M., Barnetche, T., Truchetet, M.-E., and Schaeverbeke, T. (2015). Immune related adverse events associated with anti-CTLA-4 antibodies: systematic review and meta-analysis. BMC Med. *13*, 211.

Chesney, J., Collichio, F., Andtbacka, R.H.I., Puzanov, I., Glaspy, J., Milhem, M., Hamid, O., Cranmer, L., Saenger, Y., Ross, M., et al. (2016). Interim safety and efficacy of a randomized (1:1), open-label phase 2 study of talimogene laherparepvec (T) and ipilimumab (I) vs I alone in unresected, stage IIIB-IV melanoma. Ann. Oncol. *27*, 1108PD.

Chesney, J.A., Puzanov, I., Ross, M.I., Collichio, F.A., Milhem, M.M., Chen, L., Kim, J.J., Garbe, C., Hauschild, A., and Andtbacka, R.H.I. (2017). Primary results from a randomized (1:1), open-label phase II study of talimogene laherparepvec (T) and ipilimumab (I) vs I alone in unresected stage IIIB- IV melanoma. J. Clin. Oncol. *35*, 9509.

Dias, J.D., Hemminki, O., Diaconu, I., Hirvinen, M., Bonetti, A., Guse, K., Escutenaire, S., Kanerva, A., Pesonen, S., Löskog, A., et al. (2012). Targeted cancer immunotherapy with oncolytic adenovirus coding for a fully human monoclonal antibody specific for CTLA-4. Gene Ther. *19*, 988–998.

Efferson, C.L., Tsuda, N., Kawano, K., Nistal-Villán, E., Sellappan, S., Yu, D., Murray, J.L., García-Sastre, A., and Ioannides, C.G. (2006). Prostate tumor cells infected with a recombinant influenza virus expressing a truncated NS1 protein activate cytolytic CD8+ cells to recognize noninfected tumor cells. J. Virol. *80*, 383–394.

Engeland, C.E., Grossardt, C., Veinalde, R., Bossow, S., Lutz, D., Kaufmann, J.K., Shevchenko, I., Umansky, V., Nettelbeck, D.M., Weichert, W., et al. (2014). CTLA-4 and PD-L1 checkpoint blockade enhances oncolytic measles virus therapy. Mol. Ther. *22*, 1949–1959.

Fransen, M.F., van der Sluis, T.C., Ossendorp, F., Arens, R., and Melief, C.J.M. (2013). Controlled local delivery of CTLA-4 blocking antibody induces CD8+ T-cell-dependent tumor eradication and decreases risk of toxic side effects. Clin. Cancer Res. *19*, 5381–5389.

Fulton, B.O., Palese, P., and Heaton, N.S. (2015). Replication-Competent Influenza B Reporter Viruses as Tools for Screening Antivirals and Antibodies. J. Virol. *89*, 12226–12231.

García-Sastre, A., Egorov, A., Matassov, D., Brandt, S., Levy, D.E., Durbin, J.E., Palese, P., and Muster, T. (1998). Influenza A virus lacking the NS1 gene replicates in interferon-deficient systems. Virology *252*, 324–330.

Grimm, D., Staeheli, P., Hufbauer, M., Koerner, I., Martínez-Sobrido, L., Solórzano, A., García-Sastre, A., Haller, O., and Kochs, G. (2007). Replication fitness determines high virulence of influenza A virus in mice carrying functional Mx1 resistance gene. Proc. Natl. Acad. Sci. USA *104*, 6806–6811.

Hamilton, J.R., Sachs, D., Lim, J.K., Langlois, R.A., Palese, P., and Heaton, N.S. (2016). Club cells surviving influenza A virus infection induce temporary nonspecific antiviral immunity. Proc. Natl. Acad. Sci. USA *113*, 3861–3866.

He, W., Mullarkey, C.E., and Miller, M.S. (2015). Measuring the neutralization potency of influenza A virus hemagglutinin stalk/stem-binding antibodies in polyclonal preparations by microneutralization assay. Methods *90*, 95–100.

Heaton, N.S., Leyva-Grado, V.H., Tan, G.S., Eggink, D., Hai, R., and Palese, P. (2013). In vivo bioluminescent imaging of influenza a virus infection and characterization of novel cross-protective monoclonal antibodies. J. Virol. *87*, 8272–8281.

Hock, K., Laengle, J., Kuznetsova, I., Egorov, A., Hegedus, B., Dome, B., Wekerle, T., Sachet, M., and Bergmann, M. (2017). Oncolytic influenza A virus expressing interleukin-15 decreases tumor growth in vivo. Surgery *161*, 735–746.

Kleinpeter, P., Fend, L., Thioudellet, C., Geist, M., Sfrontato, N., Koerper, V., Fahrner, C., Schmitt, D., Gantzer, M., Remy-Ziller, C., et al. (2016). Vectorization in an oncolytic vaccinia virus of an antibody, a Fab and a scFv against programmed cell death -1 (PD-1) allows their intratumoral delivery and an improved tumor-growth inhibition. OncoImmunology *5*, e1220467.

Kuzu, O.F., Nguyen, F.D., Noory, M.A., and Sharma, A. (2015). Current State of Animal (Mouse) Modeling in Melanoma Research. Cancer Growth Metastasis *8* (*Suppl 1*), 81–94.

Lindenmann, J., and Klein, P.A. (1967). Viral oncolysis: increased immunogenicity of host cell antigen associated with influenza virus. J. Exp. Med. *126*, 93–108.

Moore, A.E. (1949). Effect of inoculation of the viruses of influenza A and herpes simplex on the growth of transplantable tumors in mice. Cancer *2*, 516–524.

Muster, T., Rajtarova, J., Sachet, M., Unger, H., Fleischhacker, R., Romirer, I., Grassauer, A., Url, A., García-Sastre, A., Wolff, K., et al. (2004). Interferon resistance promotes oncolysis by influenza virus NS1-deletion mutants. Int. J. Cancer *110*, 15–21.

Overwijk, W.W., and Restifo, N.P. (2001). B16 as a mouse model for human melanoma. Curr. Protoc. Immunol. *Chapter 20*, Unit 20.1.

Pena, L., Sutton, T., Chockalingam, A., Kumar, S., Angel, M., Shao, H., Chen, H., Li, W., and Perez, D.R. (2013). Influenza viruses with rearranged genomes as live-attenuated vaccines. J. Virol. *87*, 5118–5127.

Puzanov, I., Milhem, M.M., Minor, D., Hamid, O., Li, A., Chen, L., Chastain, M., Gorski, K.S., Anderson, A., Chou, J., et al. (2016). Talimogene Laherparepvec in Combination With Ipilimumab in Previously Untreated, Unresectable Stage IIIB-IV Melanoma. J. Clin. Oncol. *34*, 2619–2626.

Russell, S.J., Peng, K.-W., and Bell, J.C. (2012). Oncolytic virotherapy. Nat. Biotechnol. *30*, 658–670.

Sandin, L.C., Eriksson, F., Ellmark, P., Loskog, A.S., Tötterman, T.H., and Mangsbo, S.M. (2014). Local CTLA4 blockade effectively restrains experimental pancreatic adenocarcinoma growth in vivo. OncoImmunology *3*, e27614.

Simmons, A.D., Moskalenko, M., Creson, J., Fang, J., Yi, S., VanRoey, M.J., Allison, J.P., and Jooss, K. (2008). Local secretion of anti-CTLA-4 enhances the therapeutic efficacy of a cancer immunotherapy with reduced evidence of systemic autoimmunity. Cancer Immunol. Immunother. *57*, 1263–1270.

Tan, G.S., Lee, P.S., Hoffman, R.M.B., Mazel-Sanchez, B., Krammer, F., Leon, P.E., Ward, A.B., Wilson, I.A., and Palese, P. (2014). Characterization of a broadly neutralizing monoclonal antibody that targets the fusion domain of group 2 influenza A virus hemagglutinin. J. Virol. *88*, 13580–13592.

Tran, V., Moser, L.A., Poole, D.S., and Mehle, A. (2013). Highly sensitive real-time in vivo imaging of an influenza reporter virus reveals dynamics of replication and spread. J. Virol. *87*, 13321–13329.

Tuve, S., Chen, B.-M., Liu, Y., Cheng, T.-L., Touré, P., Sow, P.S., Feng, Q., Kiviat, N., Strauss, R., Ni, S., et al. (2007). Combination of tumor site-located CTL-associated antigen-4 blockade and systemic regulatory T-cell depletion induces tumor-destructive immune responses. Cancer Res. *67*, 5929–5939.

van Rikxoort, M., Michaelis, M., Wolschek, M., Muster, T., Egorov, A., Seipelt, J., Doerr, H.W., and Cinatl, J., Jr. (2012). Oncolytic effects of a novel influenza A virus expressing interleukin-15 from the NS reading frame. PLoS ONE *7*, e36506.

Weber, J. (2007). Review: anti-CTLA-4 antibody ipilimumab: case studies of clinical response and immune-related adverse events. Oncologist *12*, 864–872.

Zamarin, D., Holmgaard, R.B., Subudhi, S.K., Park, J.S., Mansour, M., Palese, P., Merghoub, T., Wolchok, J.D., and Allison, J.P. (2014). Localized oncolytic virotherapy overcomes systemic tumor resistance to immune checkpoint blockade immunotherapy. Sci. Transl. Med. *6*, 226ra32.

Cell Reports, Volume *22*

Supplemental Information

A Recombinant Antibody-Expressing Influenza Virus Delays Tumor Growth in a Mouse Model

Jennifer R. Hamilton, Gayathri Vijayakumar, and Peter Palese

Supplemental Experimental Procedures

Plasmids and rescue of recombinant antibody-expressing influenza viruses

PB1-9H10$_{\text{heavy chain}}$ and PA-9D9$_{\text{light chain}}$ were cloned into the ambisense cloning vector pDZ between bidirectional promoters that transcribe both vRNA and mRNA for viral rescue, as previously described (Grimm et al., 2007). To prevent duplication of packaging sequences within the PB1 and PA vRNA segments, silent mutations within the terminal 117 bp of PB1 or 123 bp of PA (as described by Gao *et al.*, (2010) A nine-segment influenza A virus carrying subtype H1 and H3 hemagglutinins. J. Virol. *84*, 8062–71.) were utilized, and the unmodified packaging sequences were duplicated downstream of the antibody genes. The 2A sequence from Porcine teschovirus 1 (GSGATNFSLLKQAGDVEENPGP) was used to promote co-translational separation of the polymerase and antibody proteins. The human IL-2 signal sequence (MYRMQLLSCIALSLALVTNS) was used to target the translation of the antibody nascent polypeptide into the secretory pathway (see figure 1 for diagram).

The 9H10 IgG2a antibody sequence (Tan et al., 2014) was codon optimized (http://genomes.urv.es/OPTIMIZER/) to match the codon usage of influenza virus (http://www.kazusa.or.jp/codon/cgi-bin/showcodon.cgi?species=465364) and the transgenic regions of the PB1-9H10$_{\text{heavy chain}}$ and PA-9D9$_{\text{light chain}}$ were synthesized (Integrated DNA Technologies).

PB1 and PA with codon switched packaging sequences (as described by Gao *et al.*, (2010) A nine-segment influenza a virus carrying subtype H1 and H3 hemagglutinins. J. Virol. *84*, 8062–71.) and the synthesized transgenic regions were amplified via PCR. Primers were designed to encode 18 nucleotides of homology between the appropriate PCR products, which were inserted into SapI-digested pDZ plasmid via recombination-based Infusion HD cloning (Takara Bio Inc). All plasmids generated were sequenced verified prior to viral rescue.

The PB1-9H10$_{\text{heavy chain}}$ and PA-9D9$_{\text{light chain}}$ pDZ plasmids were introduced into 293T cells using LT-1 transfection reagent (Mirus) along with the six pDZ plasmids encoding the remaining viral segments. 48 hours post transfection, supernatant of the transfected cells was injected into 10-day old specific pathogen free (SPF) eggs (Charles River) and virus was amplified at 33°C for 3-days prior to allantoic fluid isolation. Rescued viruses were dilution purified in eggs prior to the growth of viral stocks.

The same strategy was used to engineer and rescue IAV-CTLA4, which expresses the 9D9 scFv from both PB1 and PA segments. The 9D9 scFv sequence was obtained from the US 20110044953 A1 patent application (Inventors: Drs. James Allison and Michael Curran), and codon optimized to match the IAV genome, as described above.

Viability assays

To assay the viability following IAV infection, $5x10^4$ B16-F10 cells were plated per well in 12-well plates. Virus was diluted in infection media, as described previously (Hamilton et al., 2016), and 200ul was used to infect for 1 hour at 37°C. The inoculum was then aspirated, and 1 ml media was added back per well. Media was aspirated and 200ul of PBS+200ul Cell Titer Glo

(Promega) was added to each well 48 HPI. Plates were agitated on an orbital shaker for 2 minutes at room temperature (RT), followed by a 15-minute incubation in the dark. The luciferase activity of each well was quantified and samples were collected in quadruplicates.

RT-PCR and vRNA isolation

Viral stocks were mixed in equal volume (0.5ml) with RLT buffer and passed through QIAshredder at 8000 x g (QIAGEN). Flow-through was mixed with 0.5ml 70% ethanol and viral RNA was extracted following the RNeasy protocol (QIAGEN) and eluted in 30ul of Ultrapure DNAse and RNAse-free water (Thermo Fisher). RT-PCR was performed with Superscript III One-Step RT-PCR System with Platinum Taq (Thermo Fisher). cDNA was synthesized at 60°C for 30 minutes and RT-PCR reactions were supplemented with 5% DMSO (Sigma) The transgenic region of PA was amplified using 5'-GCAGGACTTTATTAGCAAAGTCGGT-3' and 5'-AGTAGAAACAAGGTACTTTTTTGGA-3' primers, and the transgenic region of PB1 was amplified using 5'-CCATCTTGAATACAAGTCAAAGAGG-3' and 5'-AGTAGAAACAAGGCATTTTTTCATG-3' primers.

Protein G purification of antibodies

To isolate 9H10 from IAV-Ab infected eggs, 10^{-7} dilution of IAV-Ab was performed in PBS and 100ul was injected per 10-day old SPF egg. Eggs were incubated at 33°C for 72-96 hours and then allantoic fluid was isolated, pooled, filtered through a vacuum 0.22um filter (Falcon), and applied to a 1.5 x 30cm chromatography column (Bio-Rad) packed with Protein G/Agarose (Invivogen). Flow-through was collected and re-applied to the column. Following antibody capture, the column was washed 2x with PBS and antibody was eluted with 45ml of 0.1 M glycine, pH 2.7 into 5ml of Tris-HCl pH 10. Antibody was concentrated and buffer was exchanged to PBS using an Amicon Ultra-15 filter unit (EMD Millipore) and concentration was quantified via NanoDrop (Thermo Fisher).

ELISA

ELISA plates (Thermo Fisher) were coated with A/X-31 H3N2 virus (diluted 1:5 in PBS) at 4°C overnight and then blocked with 1% BSA in PBS for 2 hours at RT. Samples were applied and plates incubated overnight at 4°C or for 1 hour at RT. Plates were then washed 3x with PBS, and incubated with anti-mouse HRP-conjugated secondary antibody (GE Healthcare Life Sciences) for 30 minutes. Plates were developed with SigmaFAST OPD (Sigma) and read on a FilterMax F3 Multi-Mode Microplate Reader (Molecular Devices) at 450nm. A standard curve was generated for each plate using known concentrations of hybridoma-produced 9H10 antibody, which was subsequently used to interpolate unknown concentrations using a 4-parameter non-linear regression in Prism (GraphPad).

Microneutralization assays

MDCK cells were plated at $3x10^4$ cells per well in 96-well plates. Twenty-four hours later, 2-fold dilutions of antibody aliquots were performed and each dilution was mixed with 100 pfu X-31 in 1x MEM media (Gibco) and incubated for 1 hour at room temperature. The virus/antibody mix was then added to MDCK cells and incubated for 1 hour at 37°C. The virus/antibody mix was then aspirated and replaced with 1x MEM containing the appropriate antibody dilution. A neutralizing, anti-PR8 HA antibody (PY102) was added to all wells at a concentration of 30ug/ml to neutralize any IAV-9H10 present in the $9H10_{IAV}$ antibody aliquot.

Viral infections

For *in ovo* viral growth curves, virus was diluted to 1000pfu/ml in PBS and 100ul was injected per egg. Eggs were incubated at 33°C, 5 eggs per time point. For *in vitro* viral growth curves, virus was diluted to an MOI=0.01 in 300ul and $5x10^4$ B16-F10 cells were infected in 6-well plates. Following virus absorption for 1hr at 37°C, inoculum was removed and replaced with OPTI-MEM (Gibco) supplemented with 3% BSA and Pen/Strep, with or without TPCK-treated trypsin (Sigma) at a final concentration of 1ug/ml. Samples were taken in triplicate. All viral samples were titrated via standard plaque assay on MDCK cells.

To quantify the amount of antibody produced following IAV-9H10 infection of B16-F10 cells, approximately $6.7x10^6$ cells were infected at an MOI = 5 and the quantity of 9H10 antibody in the supernatant was measured 48 hours post infection. Samples were collected in triplicate. All viral samples were titrated via standard plaque assay on MDCK cells.